

Thermally induced two-phase oscillating flow in a capillary tube: theoretical and experimental investigations

Manoj Rao, Frédéric Lefèvre*, Jocelyn Bonjour

Centre de Thermique de Lyon, UMR 5008 CNRS-INSA-UCB
INSA, 20 av. A. Einstein, 69621 Villeurbanne Cedex – France

Tel.: +33 4 7243 8251; fax: +33 4 7243 8811.

E-mail address: frederic.lefevre@insa-lyon.fr (F. Lefèvre)

Sameer Khandekar

Department of Mechanical Engineering,
Indian Institute of Technology Kanpur, Kanpur (UP) 208016 India

ABSTRACT

This paper deals with thermally-induced oscillations of a meniscus in a two-phase system consisting of a liquid plug and a vapor bubble in a capillary tube of circular cross-section. This system represents the simplest version of a pulsating heat pipe (PHP). An experimental setup, made as entirely transparent to enable the observation of the meniscus oscillations, has been used to visualize the oscillations. The results are compared to a mathematical model based on the balance equations. In the model, the evaporation of a thin film left by the meniscus when it leaves the evaporator is taken into account. The presence and the evaporation of this thin film have been observed experimentally. Results from the proposed model show a good agreement with the experiment.

KEY WORDS: pulsating heat pipe, oscillating flow, thin film

1. INTRODUCTION

Research on Pulsating Heat Pipes (PHP) has received substantial attention in the recent past, due to its unique operating characteristics and potential applications in many passive heat transport situations (Zhang & Faghri 2008; Khandekar et al. 2010). A PHP is a capillary tube (with no wick structure) bent into many turns and partially filled with a working fluid. When the temperature difference between the heat source and the heat sink exceeds a certain threshold, the gas bubbles and liquid plugs begin to oscillate back and forth. The heat is thus transferred not only by the latent heat exchange like in other types of heat pipes, but also by sensible heat transfer between the wall and the fluid.

Compared to other cooling solutions, PHPs are simple and thus more reliable and cheap. However, there is no theoretical model or correlation that would predict the PHP behavior and heat exchange at present. This prevents the PHPs from being used industrially. Reliable design tools can only be formulated if the nuances of its operating principles are well understood; at present, this is rather insufficient for framing comprehensive models.

In this context several authors have focused their efforts on the simplest pulsating heat pipe consisting of one liquid plug and one vapor bubble. Mathematical model based on the balance equations were developed for this simple system (Zhang & Faghri 2002; Dobson 2005). The vapor-phase was considered as an ideal gas. The pressure fluctuations inside the system was introduced by modeling the evaporation of a thin liquid film left on the wall when the liquid plug leaves the evaporator.

Recently (Das et al. 2010) presented the first experimental results of such a system consisting in a 2.0 mm ID capillary tube, heated on one hand and cooled on the other end. They were able to obtain oscillations in this system in a definite range of experimental conditions. Vapour pressure was recorded. The oscillation of the liquid slug was observed but only in the condenser section. A satisfactory quantitative agreement was found between these experimental data and the results of an improved version of the mathematical models previously described. Nevertheless improvements were needed to increase the quality of the experimental results.

This paper presents experimental data obtained with an improved version of this bench. The objective of this new bench is to increase the understanding of the basic phenomena involved in thermally-induced two-phase oscillatory flows. Compared to the previous set-up (Das et al. 2010), the new design of the experimental bench is entirely transparent in order to observe the liquid film dynamics in the condenser but also in the evaporator, while the evaporator, made of copper, was opaque in the previous experiment. Furthermore, the tube is in vertical position, while it was in horizontal position in the previous experiment. Finally, the set-up has been improved in order to remove the singularities between the tube and the reservoir. Thus, the inner of the capillary tube is perfectly smooth and in a straight line from the evaporator to the reservoir.

Some preliminary experimental results are presented for pentane as working fluid. The results are compared to a mathematical model.

2. EXPERIMENTAL SET-UP

The experimental set-up is presented in Figure 1. It is an improved version of a previous experiment presented by Das et al. (2010). It consists of a very basic PHP with one liquid plug and one vapor bubble in a vertical capillary tube of circular cross-section. The transparent capillary tube, made of glass, is closed at one side and connected to a reservoir maintained at a constant pressure at the other side. Its inner diameter is 2 mm. The liquid plug oscillates between a heat source (evaporator section length = 20 cm) located near the closed side and a heat sink (condenser section length = 20 cm) located near the reservoir. In between, an adiabatic section separates the condenser and the evaporator (length = 1 cm). The evaporator and the condenser are transparent heat exchangers, whose temperature is controlled by means of two thermostatic baths. A third thermostatic bath is used to control the temperature of the reservoir, and thus its pressure.

The two-phase oscillatory flow is characterized by vapour pressure measurements as well as meniscus displacement measurements. An absolute pressure sensor (supplied by M/s KISTLER®, piezo-resistive sensor type 4005B, operating range of 0-5 bar) is located at the closed end of the tube and a high speed camera (Fastcam-1024 PCI, 3000 frames/s) is used to record the meniscus displacement. Another tube which comes out of the

evaporator end is connected to a reservoir at vacuum, with an isolation valve in between. This tube connected with the vacuum reservoir serves two purposes. It helps to remove any non-condensable gases present in the capillary tube before charging the device. Second, it helps control the position of the liquid-vapor meniscus in the beginning of the experiment.

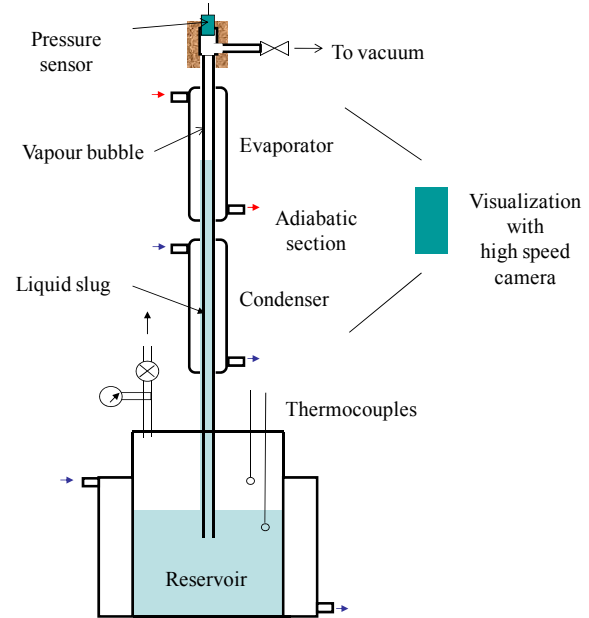


Figure 1: Experimental set-up.

Before the experiments, the system is completely evacuated to remove the non-condensable gases. The reservoir is then filled with the working fluid (Pentane).

3. EQUATIONS OF THE MODEL

This section presents the modeling of the system consisting of a vapor plug and a liquid slug oscillating in a tube closed at one end and connected to a reservoir at a constant pressure P_r at the other end (Figure 2). The equations of the model were already presented in Das et al. (2010). Some modifications are introduced in this paper to take into account the peculiarities of the new experimental set-up.

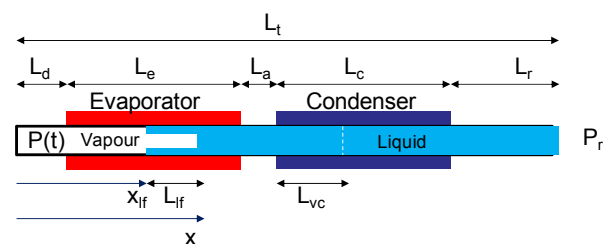


Figure 2: Geometrical properties considered in the model.

The liquid plug confines a vapour bubble at the closed end of a cylindrical tube of diameter d and cross-section area $S = \pi d^2/4$. The x axis reference is located at the closed end of the tube. The length of the tube is L_t . A dead volume is introduced in the model to take into account the volume of vapour trapped between the evaporator and the end of the tube. This dead volume is due to the presence of the pressure sensor and the connection to the vacuum reservoir. It is modeled by an equivalent length L_d . The evaporator length is L_e and the evaporator tube wall is maintained at a constant temperature T_e . The condenser length is L_c and the condenser tube wall is maintained at a constant temperature T_c . The condenser and the evaporator are separated by an adiabatic length L_a . A part L_r of capillary tube extends beyond the condenser until the reservoir at a constant pressure P_r . The pressure of the vapor bubble inside the tube P is a function of time.

When the liquid plug leaves the evaporator, a small liquid film is left on the wall. This film is responsible for a huge amount of evaporation. The thickness δ_{lf} of this film is supposed to be constant but its length L_{lf} is not constant due to evaporation or rewetting of the liquid slug, when it enters into the evaporator. The location of this film inside the evaporator is x_{lf} .

When the liquid slug is pushed into the condenser, a part of the condenser wall of length L_{vc} is in contact with the vapour and condensation occurs.

The steady state model is based on the balance equations. The momentum balance equation for the liquid slug inside the tube is written as:

$$\frac{d(m_1 u)}{dt} = (F_p + m_1 g \pm F_\tau) \quad (1)$$

where m_1 is the mass of liquid inside the tube, which is easily derived from geometrical considerations and the density of the liquid ρ . F_p is the difference of pressure acting on the liquid slug $F_p = S(P - P_r)$, u the velocity of the liquid plug, g the gravity and F_τ the sum of regular and singular friction forces acting on the liquid slug:

$$F_\tau = \frac{1}{2} C_f d \rho \pi (L_t - x) u^2 + \frac{1}{2} S \rho u^2 \quad (2)$$

The first term of the equation is related to the regular pressure drop while the second one stands for the singular pressure drop due to the contraction or the enlargement at the end of the tube. The friction coefficient C_f depends on the Reynolds number Re :

$$C_f = \begin{cases} 0 & Re = 0 \\ 16 & \text{if } Re < 1 \\ \frac{16}{Re} & \text{if } 1 < Re < 1180 \\ 0.078 Re^{-0.25} & \text{if } Re \geq 1180 \end{cases} \quad (3)$$

The velocity can be related to the location $x(t)$ of the meniscus:

$$u = \frac{dx}{dt} \quad (4)$$

The length of the liquid film L_{lf} is defined only in the evaporator section since no evaporation is supposed to occur in the adiabatic section. It is expressed by considering the mass balance equation:

$$\frac{dL_{lf}}{dt} = \begin{cases} 0 & \text{if } L_{lf} = 0 \text{ and } u < 0 \\ -\frac{1}{\rho \pi d \delta_{lf}} \dot{m}_e & \text{if } x > L_e \\ u - \frac{1}{\rho \pi d \delta_{lf}} \dot{m}_e & \text{otherwise} \end{cases} \quad (5)$$

The flow rate of evaporation is:

$$\dot{m}_e = \frac{h_e \pi d L_{lf}}{h_{lv}} (T_e - T_{sat}(P)) \quad (6)$$

where h_e is the evaporation coefficient.

A fourth equation is obtained by considering the mass balance equation for the vapour:

$$\frac{dm_v}{dt} = \dot{m}_v = (\dot{m}_e - \dot{m}_c) \quad (7)$$

where the flow rate of condensation is:

$$\dot{m}_c = \frac{h_c \pi d L_c}{h_{lv}} (T_{sat}(P) - T_c) \quad (8)$$

The last equation is the energy balance equation for the volume of vapour:

$$\frac{dT}{dt} = \frac{1}{m_v C_{vv}} (\dot{m}_v R_v T + q_{\text{sens}} - P S u) \quad (9)$$

where P and T are respectively the vapor pressure and the vapor temperature. R_v is the vapor gas constant and C_{vv} the vapor specific heat at constant volume. The sensible heat flux q_{sens} is given by:

$$q_{\text{sens}} = h_{\text{sens}} (T_e - T) \quad (10)$$

where h_{sens} is the sensible heat transfer coefficient. The vapor is defined by the equation of state which is assumed to be that of ideal gas:

$$P = \frac{m_v R_v T}{S x} \quad (11)$$

Equations 1, 4, 5, 7 and 9 forms a set of five coupled differential equations which five unknowns x , u , L_{lf} , m_v and T . These equations are solved using a fourth-order Runge-Kutta method. More details on the resolution process can be found in Das et al. (2010).

4. COMPARISON OF THE MODEL WITH THE EXPERIMENTAL DATA

Preliminary experimental data obtained with pentane as working fluid are presented in this part and compared to the mathematical model. The temperature of the reservoir is equal to 12 °C. The related saturation pressure is equal to 0.42 bars. The temperature of the condenser is constant and equal to -11.5 °C. Figure 3 presents the pressure variations for two different evaporator temperature ($T_e = 21$ °C and $T_e = 26$ °C) during a period of 10 s. For evaporator temperatures lower than 21 °C, it was not possible to sustain the oscillations. Above a temperature of 26 °C, the oscillations were somewhat chaotic due to nucleation inside the liquid plug at the evaporator.

Figure 4 presents the location of the meniscus versus time in the same experimental conditions. It has to be noted that for this preliminary experiment the pressure transducer and the high speed camera are not synchronized. Thus, the results of Figure 3 can only be qualitatively compared to results of Figure 4. Figure 5 focuses on one period of both the pressure oscillations and location of the meniscus.

The oscillation shape is periodic but not sinusoidal. The frequency is close to 2 Hz for both evaporator temperatures. The repetitive period is made of two oscillations: one small for which the meniscus does not enter into the evaporator and one large where the meniscus enters into the evaporator.

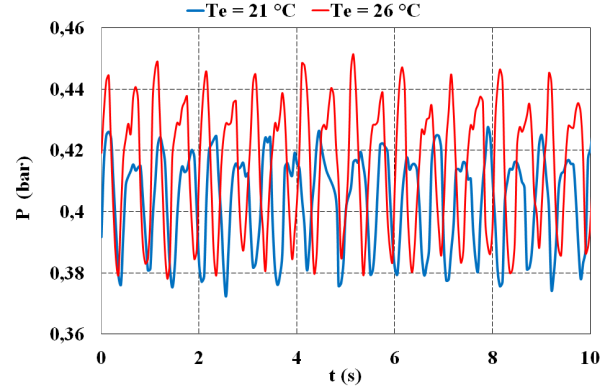


Figure 3: Experimental pressure variation
 $T_c = -11.5$ °C and $T_r = 12$ °C

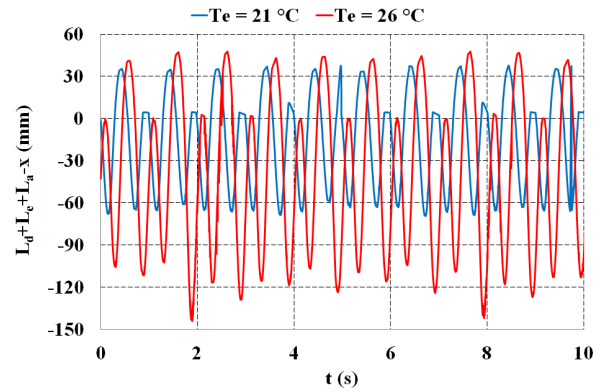


Figure 4: Experimental location of meniscus
 $T_c = -11.5$ °C and $T_r = 12$ °C

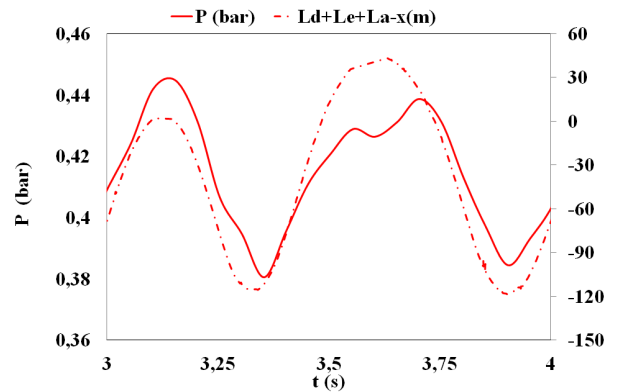


Figure 5: Experimental pressure and location of the meniscus during one period; $T_e = 26$ °C

The pressure maximum amplitude is equal to 0.07 (peak to peak) bars for $T_e = 26$ °C and 0.05 (peak to peak) bars for $T_e = 21$ °C. When the meniscus enters the evaporator, we observe a small

discontinuity in the pressure increase. At the same time, the meniscus location is at its maximum deep into the evaporator. Then the pressure increases again while the meniscus begins to leave the evaporator. This behavior can be explained by modifications in the evaporation of the thin film. When the meniscus is deep into the evaporator the length of the thin film is equal to zero, evaporation stops and thus the pressure variation is smooth. On the contrary, when the meniscus leaves the evaporator, a thin film is left, which creates a huge amount of evaporation and is responsible for the pressure increase.

The evaporator temperature has a huge influence on the oscillation amplitude. The meniscus location maximum amplitude is nearly equal to 20 cm for $T_e = 26\text{ }^\circ\text{C}$ and almost 10 cm for $T_e = 21\text{ }^\circ\text{C}$. It is important to note that this set-up enables to observe the thin film and its evaporation, which is an important point, since the evaporation of this film is the bases of the mathematical model. Since the evaporator was opaque in the previous experimental set-up (Das et al. 2010), this observation was not possible.

Figure 6 to Figure 8 presents the results of the mathematical in the same conditions as the experimental set-up. The geometrical parameters introduced in the model are similar to the experimental set-up. The length of the dead volume L_d is estimated to 30 cm. This length is relatively important compare to evaporator length, which is due to the presence of the pressure transducer and the valve connected to the vacuum reservoir. The length L_r is equal to 24 cm. In the purpose of comparison with the experimental data some unknown parameters have to be estimated to fit at best the experimental data. The thickness of the liquid film is equal to $15\text{ }\mu\text{m}$, the evaporator and condenser heat transfer coefficients are equal to $600\text{ W/m}^2\cdot\text{K}$ and $200\text{ W/m}^2\cdot\text{K}$ respectively. The sensible heat transfer coefficient in the evaporator is equal to $30\text{ W/m}^2\cdot\text{K}$. All the parameters are the same for both experimental data except the temperature of the evaporator.

The results show that the mathematical model is able to reproduce the physical behavior observed experimentally. This is mostly true for the repetitive period, which is made of one small oscillation followed by a large one, for which the pressure variation shape is very similar to the one observed experimentally.

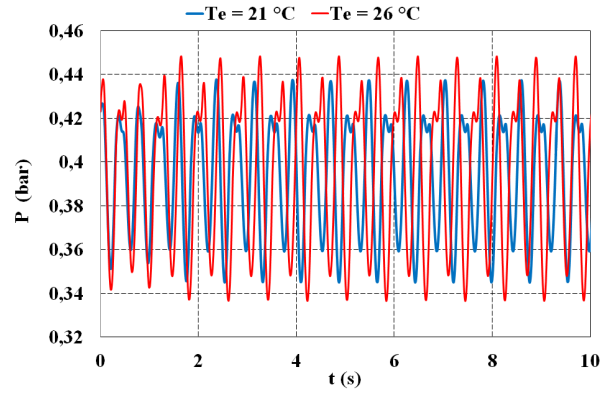


Figure 6: Numerical pressure variation
 $T_c = -11.5\text{ }^\circ\text{C}$ and $T_r = 12\text{ }^\circ\text{C}$

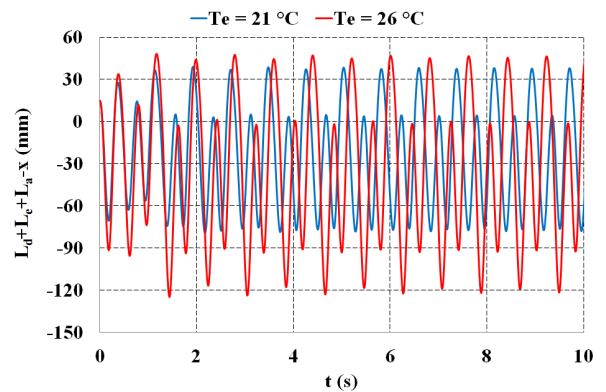


Figure 7: Numerical location of meniscus
 $T_c = -11.5\text{ }^\circ\text{C}$ and $T_r = 12\text{ }^\circ\text{C}$

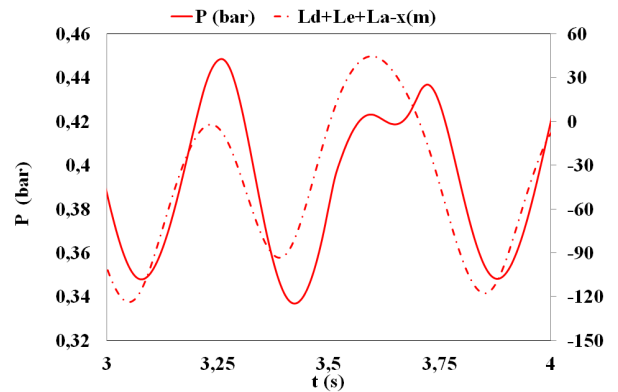


Figure 8: Numerical pressure and location of the meniscus during one period; $T_e = 26\text{ }^\circ\text{C}$

The main discrepancies are observed in the pressure amplitude, which are equal to 0.11 bar and 0.09 bar for $T_e = 26\text{ }^\circ\text{C}$ and $T_e = 21\text{ }^\circ\text{C}$, respectively. This is almost 40 % higher than that measured experimentally. Amplitude variations for both the pressure and the location of the meniscus are mostly controlled by the pressure drops inside the tube as well as the heat transfer coefficient of condensation and evaporation. Even if the sensible

heat transfer for the vapor has been introduced in the model, it is a second-order parameter.

The other discrepancy is the frequency, which is equal to 2.6 Hz numerically. The frequency of the oscillations is mainly due to the mass of vapor and liquid inside the tube. As an illustration, in the previous set-up (Das et al. 2010), the frequency was twice that observed in the present experiment, but the evaporator length and the dead volume were much smaller (~15 cm).

5. CONCLUSIONS AND PERSPECTIVES

These preliminary results are very promising. Some important parameters have still to be estimated to fit with the experimental data. At the moment, we are able to observe the presence and the evaporation of the thin liquid film, but it would be necessary to measure its thickness. Confocal microscopy could be used for that purpose, as it has already been used successfully to measure the meniscus curvature radius in the grooved capillary structure of a flat plate heat pipe but also the condensation film on the fins with thicknesses down to 2 μm (Lefèvre et al. 2010). The dead volume has to be reduced since it contributes to reduce the frequency of the oscillation and thus it is important to limit as much as possible its impact. One of the actual limitations of our approach is that the different heat transfer coefficients have also to be estimated. As their sensibility to the model is correlated to that of the pressure drops, it would be necessary to estimate accurately the pressure drops in such an oscillating device. It is planned to measure this pressure drops using the same set-up in adiabatic conditions, using a mechanical pressure oscillator. The temperature of both the evaporator and the condenser are supposed to be equal to the temperature imposed by each of the thermostatic bathes. However, heat conduction in the transparent wall is not taken into account in the equation, which could modify the numerical conditions. Finally, temperature measurement of the vapor would be capital information, but this measurement is difficult due to the high frequency of the oscillations compare to the time response of the temperature sensor, and also radiative heat transfer between the wall and the sensor.

NOMENCLATURE

C_f	friction coefficient
C_v	specific heat at constant volume (J/kg.K)
d	tube diameter (m)
g	gravity (m/s^2)

h	heat transfer coefficient ($\text{W/m}^2\text{.K}$)
h_{lv}	latent heat of evaporation (J/kg)
L	Length (m)
m	mass (kg)
P	pressure (Pa)
q	heat flux (W/m^2)
Re	Reynolds number
R_v	vapour gas constant (J/kg.K)
S	tube section (m^2)
t	time (s)
T	temperature ($^{\circ}\text{C}$)
u	velocity (m.s^{-1})
x	location of the meniscus (m)
Greek letters	
δ	film thickness
μ	dynamic viscosity (Pa.s)
ρ	density (kg.m^{-3})
Subscripts	
a	adiabatic
e, c	evaporator, condenser
d	dead volume
f	film
l, v	liquid, vapour
r	reservoir
sat	saturation
sens	sensible
t	total

ACKNOWLEDGEMENT

Financial support from the Indo-French Centre for the Promotion of Advanced Research, New Delhi (Project #: 4408-1/2010), under the aegis of Indian Department of Science and Technology and the French Ministry of Foreign Affairs and from Bhabha Atomic Research Center, Department of Atomic Energy, Government of India, is gratefully acknowledged.

REFERENCES

- Das, S. et al., 2010. Thermally induced two-phase oscillating flow inside a capillary tube. *International Journal of Heat and Mass Transfer*, 53(19-20), p.3905–3913.
- Dobson, R.T., 2005. An open oscillatory heat pipe water pump. *Applied Thermal Engineering*, 25(4), p.603–621.
- Khandekar, S. et al., 2010. Local hydrodynamics of flow in a pulsating heat pipe: a review. *Frontiers in Heat Pipes*, 1.
- Lefèvre, F. et al., 2010. Confocal Microscopy for Capillary Film Measurements in a Flat Plate Heat Pipe. *Journal of Heat Transfer*, 132(3), p.031502.
- Zhang, Y. & Faghri, A., 2002. Heat transfer in a pulsating heat pipe with open end. *Int. J. Heat Mass Transfer*, 45, p.755–764.
- Zhang, Yuwen & Faghri, Amir, 2008. Advances and Unsolved Issues in Pulsating Heat Pipes. *Heat Transfer Engineering*, 29(1), p.20–44.